

RESEARCH

Open Access



Multifunctional CuO nanoparticles with enhanced photocatalytic dye degradation and antibacterial activity

Kanika Dulta¹, Gözde Koşarsoy Ağçeli², Parveen Chauhan¹, Rohit Jasrotia³, P. K. Chauhan^{1*} and Joshua O. Ighalo^{4,5}

Abstract

Rhizome extract of *Bergenia ciliata* was used as a bio-functional reducing material for the green synthesis of copper oxide nanoparticles (CuO NPs). CuO NPs were characterized using ultraviolet–visible spectroscopy, Fourier transforms infrared spectroscopy, X-ray diffraction (XRD), dynamic light scattering, scanning electron microscopy (SEM) and energy-dispersive X-ray analysis (EDX). XRD analysis revealed the monoclinic phase of synthesized CuO NPs with an average particle size of 20 nm. Spherical shaped nanoscale CuO particles were observed by EDX and SEM confirming the Cu and O presence in the synthesized NPs. CuO NPs showed antibacterial effects against *Bacillus subtilis*, *Staphylococcus aureus*, *Escherichia coli*, *Salmonella typhi*. The antioxidant effect was measured and IC₅₀ values for 2,2'-azino-bis (3-ethylbenzothiazoline-6-sulfonic acid (ABTS), 2,2-diphenyl-1-picrylhydrazyl and Ferric reducing antioxidant power assays were found to be 91.2, 72.4 and 109 µg mL⁻¹ respectively. Under sunlight, the CuO NPs reported extraordinary photocatalytic activity against Methylene Blue and Methyl Red degradation with efficiencies of 92–85%. CuO NPs have excellent potential application for the photocatalytic degradation of organic pollutants and in the development of antibacterial materials. This study offers new insights in the field of inexpensive and green synthesis-based antimicrobial effective CuO photocatalysts from *B. ciliata* to remove harmful dyes from industrial-based waters with high degradation efficiency, which is environmentally friendly.

Keywords: *Bergenia ciliata*, Copper oxide, Nanoparticle, Antimicrobial, Photocatalytic

1 Introduction

Nanotechnology is one of the most important research areas in material science. This field is remarked as a rapidly growing field of science and engineering as important researches are carried out [1]. Nanomaterials have an important place in many areas owing to their thermal properties, surface areas, particle size, and electrical conductivity [2]. Nanoparticles (NPs), which are part of nanomaterials, have many uses in the food, pharmaceutical, energy industry, biotechnology and biomedicine [3]. Different chemical and physical methods are used for the production of metallic NPs. High toxic substances

and unnecessary energy consumption in these methods are not acceptable. For this reason, green chemistry and bioprocesses have been developed for the NP synthesis to be carried out in a reliable, environmentally friendly, economical and biocompatible manner [4]. Biosynthesis using fungi, bacteria and plants and green chemistry open new horizons in NPs production. Plants with regions such as leaves, gum and fruit are also involved in metal NPs synthesis and used in antimicrobial, anticancer, antioxidant, nanomedicine, and diagnostic studies. Alkaloids, flavonoids and other natural compounds, plants function as powerful reducers and stabilizers [5]. When we look at the copper nanoparticles (CuO NPs), it draws attention among other metal oxide NPs in many applications (e.g., optics, antimicrobial, catalytic, etc.). In addition, its cost and availability are more advantageous

* Correspondence: chauhanbiochem084@gmail.com

¹Faculty of Applied Sciences and Biotechnology, Shoolini University, Solan 173229, India

Full list of author information is available at the end of the article



© The Author(s). 2021 **Open Access** This article is licensed under a Creative Commons Attribution 4.0 International License, which permits use, sharing, adaptation, distribution and reproduction in any medium or format, as long as you give appropriate credit to the original author(s) and the source, provide a link to the Creative Commons licence, and indicate if changes were made. The images or other third party material in this article are included in the article's Creative Commons licence, unless indicated otherwise in a credit line to the material. If material is not included in the article's Creative Commons licence and your intended use is not permitted by statutory regulation or exceeds the permitted use, you will need to obtain permission directly from the copyright holder. To view a copy of this licence, visit <http://creativecommons.org/licenses/by/4.0/>.

compared to Ag, Au and Pt metals. Copper has long been used antimicrobial agent, it has low toxicity and it is very important in the biomedical [6]. The metal oxide CuO NPs have demonstrated an enhanced antibacterial activity. Since nanoparticles may be smaller in size than bacterial pores, they will have a unique ability to penetrate the cell membrane, which is the case with CuO nanoparticles. Also, in some cases, this metal possesses properties better relative to the other expensive metals with antimicrobial activity, such as silver and gold. The band gap of CuO is ~ 1.7 eV and this type-p has a semiconductor feature in nonclinical structure [7]. As the simplest member of the copper compound family, CuO has many useful physical properties. It has an important place in many fields such as solar energy conversion, high-temperature superconductors, gas sensors, etc. [8]. CuO NPs are the most widely used metal NPs for wastewater treatment because of their superior catalytic properties.

Bergenia ciliata (Haw.) Sternb belongs to the family Saxifragaceae and is mostly distributed in the cold and temperate regions. It is found in traditional medicines and ayurveda for use in the treatment of different diseases and it is used in countries such as Pakistan, India, and Bhutan [9]. Lung infections, fever, diarrhoea and dissolution of kidney stones can be treated with *B. ciliata* in Indian medicine [10]. Besides, anti-tussive activity, anti-inflammatory effect, analgesic, diuretic feature, antioxidant activity, DNA protection, immunity enhancement can be achieved with this plant. *B. ciliata* has many phytochemicals (e.g., paashaanolactone, catechin, bergerin and gallic acid). Until now, NPs produced using *B. ciliata* extracts were As (Arsenic), Ag (silver), ZnO (zinc oxide) NPs. In the present work, we have adopted a green chemistry approach for the synthesis of CuO NPs from *B. ciliata* extract. The synthesis of CuO NPs using *B. ciliata* extracts was carried out for the first time in this study. The shape and size of the particles were characterized using various standard techniques. Furthermore, antioxidant, antibacterial and photocatalytic activities on Methylene Blue (MB) and Methyl Red (MR) dyes of the CuO NPs by *B. ciliata* extract are also discussed.

2 Material and methods

2.1 Collection of plant material and synthesis of CuO NPs

For the production of CuO NPs, *B. ciliata* rhizome was washed with distilled water, followed by shadow drying for 10–12 d. The dried rhizomes were ground to a fine powder and 10 g of ground powder was added to 100 mL of d-water and boiled for 10 min at 60 °C. The cooled extract was filtered through Whatman No. 1 filter paper and put into the refrigerator until it was used. Synthesis of CuO NPs by green method was carried out

by modifying the work of Sankar et al. [11]. Copper sulphate ($\text{CuSO}_4 \cdot 5\text{H}_2\text{O}$) (Himedia) was used as the precursor. 5 mM ($\text{CuSO}_4 \cdot 5\text{H}_2\text{O}$) solution of 90 mL was mixed with 10 mL filtrate and incubated at 25 °C until further colour change occurs. Colour change was evaluated by comparison with (extract and copper sulphate) the control solution to determine whether NPs were synthesized. The synthesized CuO NPs were further subjected to characterization studies.

2.2 Characterization of CuO NPs

Shimadzu UV-Vis V-530A spectrophotometer was used to measure the UV-Visible absorption spectra of the samples, which ranged from 200 to 600 nm. The Branauer-Emmet-Teller (BET) surface area of CuO NPs was measured with a AUTOSORB-6B. Prior to this measurement, the samples were degassed at 140 °C. The Fourier Transform Infrared (FTIR) spectrum (Perkin-Elmer-Spectrum Two) was obtained at a wavelength of 400–4000 cm^{-1} . Energy-dispersive X-ray analysis and elemental mapping were also performed using this device. CuO NPs X-ray Diffractometry (XRD) pattern was determined using the same instrument at Indian Institute of Technology, Mandi, using a powder X-ray diffractometer (Philips X'Pert Pro X-ray diffractometer) with Cu ($K\alpha$) radiations (1.5406 Å) in a 2θ range from 30 to 80 °C. Dynamic light scattering (DLS) analysis of CuO NPs was performed using a DynaPro Plate Reader (Wyatt Technology). Scanning electron microscopy (SEM-Hitachi/s-4200 N) was used to show the shape and morphology of CuO NPs [12].

2.3 Analysis of electrochemical study

Electrochemical study of CuO NPs synthesized using green technology was carried out on an analytical model of PalmSense 4 (Potentiostat/ Galvanostat/ Impedance Analyser) on PS Trace software. A certain amount of green synthesized CuO NPs was analysed on Dropsens (DS-110) electrodes against a bare electrode, each treated with EDC:NHS (1:1) equimolar concentration. Cyclic voltammetry analysis was performed at different scan rates (20, 40, 60 and 100 mV s^{-1}) using 2.5 mM potassium ferricyanide ($\text{K}_3[\text{Fe}(\text{CN})_6]$) redox indicator. Washing off electrodes after consecutive measurements using Phosphate Buffer Saline (pH 7.4) and Tris-EDTA (pH 8.0) as wash buffers.

2.4 Quantification of phenolic and flavonoid content

Rhizome extract of *B. ciliata* and CuO NPs were analysed for phenolic and flavonoid content using standard procedures.

2.4.1 Total phenolic content

Total phenolic content was measured using the Folin-Ciocalteu test following the updated procedure described by Singleton and Rossi [13]. For the preparation of regular extract solutions, 5 mg of each sample was dissolved in 5 mL of methanol. 1 mL Folin-Ciocalteu reagent was weighed and diluted with distilled water to form 10 mL. Each extract working standards were made by combining 1 mL standard solution with 9 mL distilled water. Each test tube was added with 1 mL of diluted Folin-Ciocalteu reagent, which was allowed to stand for 6 min, followed by the addition of distilled water and incubation for 90 min at room temperature, 10 mL of 7% sodium carbonate solution was then added to the reaction mixtures in each test tube and further diluted to 25 mL. UV spectrophotometer was used to determine the sample's absorbance at 760 nm. The equivalent milligrams of gallic acid per gram of dry sample (mg GAE g^{-1}) was used to determine the total phenolic content.

2.4.2 Total flavonoid content

Total flavonoid content was determined by the aluminium chloride colorimetric assay according to the method described by Meda et al. [14]. In 5 mL methanol, approximately 5 mg of each extract was dissolved, from each of these normal solutions, 1 mL was diluted with 9 mL distilled water and then with 1 mL NaNO_2 (5%). The mixtures were allowed to stand for 6 min for a continued reaction. Then 2 mL of 10% aluminium chloride solution was applied to each and allowed to stand for 5 min. Then the mixtures were added with 2 mL of sodium hydroxide (1 M) in series. Eventually, a UV spectrophotometer was used to measure the absorbance of the mixture at 510 nm. The total content of flavonoids was measured as milligrams of equivalent Quercetin per gram of dry sample (mg QE g^{-1}).

2.5 Antioxidant effect of CuO NPs

2.5.1 ABTS radical scavenging assay

For ABTS assay, a predefined method [15] with some modifications was performed. The ABTS radical cation solution was produced by reacting 7 mM ABTS stock solution and 2.45 mM potassium persulfate solution was prepared in 100 mL methanol. CuO NPs were added one by one with 3 mL of ABTS solution and incubated in the dark for 15 min at varying concentrations (12.5 to 100 mg L^{-1}). At 745 nm, the degree of colour changes was observed. Without any sample, the ABTS reagent was used as a control solution and ascorbic acid was used as standard. The scavenging inhibition capacity was measured;

$$\text{ABTS radical scavenging activity (\%)} = \frac{A_{\text{control}} - A_{\text{test}}}{A_{\text{control}}} \times 100$$

A_{control} : the absorbance of ABTS radical + methanol.

A_{test} : the absorbance of ABTS radical + sample/standard.

2.5.2 2,2-diphenyl-1-picrylhydrazyl (DPPH) radical scavenging assay

The DPPH assay was performed according to some modifications in predefined method [16]. For stock solution, 20 mg DPPH was dissolved in 100 methanol. Then, the DPPH solution was diluted with methanol to reach an absorbance of 0.68–0.76 at 517 nm. To prevent free radicals, the DPPH stock solution was coated with aluminum foil and kept in the dark for 24 h. CuO NPs were added one by one to 3 mL of and incubated in the dark for 15 min at different concentrations (12.5 to 100 mg L^{-1}). Without sample, DPPH methanol reagent was used as control solution and ascorbic acid used as standard.

The mixture was thoroughly prepared and held at 25 °C for 30 min in the dark. At a wavelength of 517 nm, the absorbance was determined using a spectrophotometer. The following equation was used to measure the samples' scavenging potential:

$$\text{DPPH radical scavenging activity (\%)} = \frac{A_{\text{control}} - A_{\text{test}}}{A_{\text{control}}} \times 100$$

A_{control} : the absorbance of DPPH radical + methanol.

A_{test} : the absorbance of DPPH radical + sample/standard.

The IC_{50} value, which represents the effective concentration of extract/standard required to scavenge 50% of DPPH radicals, was used to measure the scavenging behaviour of the samples.

2.5.3 Ferric reducing antioxidant power assay (FRAP)

Following Benzie and Strain's protocol, the antioxidant potential of the samples was determined spectrophotometrically [17]. The method relies on the reduction of Fe^{3+} tripyridyltriazine complex (colourless complex) to Fe^{2+} -tripyridyltriazine (blue coloured complex) by electron-donating antioxidants at low pH. The shift in absorbance at 593 nm is used to monitor this reaction.

2.6 The antimicrobial assay

Green-synthesized CuO NPs were tested on *B. subtilis*, *S. aureus*, *E. coli*, *S. typhi*. The microorganisms were procured from the Department of Food Technology of Shoolini University Solan, Himachal Pradesh, India. The antimicrobial activity was determined by the well diffusion method [18]. Individual microorganisms were cultured in 100 mL of mature broth culture for 24 h on

nutrient agar plates. Sterile cork borer was used to produce 6 mm diameter wells in a petri dish. 20 mg mL⁻¹ of plant extract and CuO NPs were used to assess the activity. The standard antibiotic Ampicillin (100 mg mL⁻¹) was used as a positive control, whereas distilled water was used as a negative control. The zone diameter was measured in millimetres after the cultures were incubated at 37 °C for 24 h. The experiment was repeated three times.

The minimum inhibitory concentration (MIC) was determined using the broth dilution method, as explained [19]. The positive and negative controls for the MIC test are 10 µL Ampicillin (100 mg mL⁻¹ stock) and 10 µL MilliQ water, respectively. 100 µL of CuO NPs (1 mg mL⁻¹) were incubated in a 96-well microtiter plate and incubated at 37 °C for 24 h. Resazurin sodium dye was added to the wells to see the results after incubation, color change from purple to pink or colorless. The lowest concentration of this color change was accepted as the MIC value of CuO NPs against the test microorganisms used in the study.

2.7 Photocatalytic activities

Under sunlight irradiation, the photocatalytic behavior of CuO NPs was analyzed for the degradation of MB and MR dyes. A beaker was filled with 10 mL (20 ppm) of dyes for the reaction, approximately (10 mg L⁻¹) of CuO NPs were added to the dye solutions as-prepared, followed by stirring of the reaction mixture for 15 min in dark. Thereafter, the reaction mixture was kept in the sunlight for up to 135 min. The experiment was conducted outside in the sunlight, with the adsorption/desorption balance being constantly stirred. After the reaction, the CuO NPs were centrifuged out of the solution, and the dye concentration was measured using the UV–Visible spectrum. After some time, the amplitude of the MB and MR absorbance peaks (at 625 and 525 nm) were measured. The concentration variance of the MB and MR solutions was calculated using the light absorption spectrum intensity, and the dye degradation was calculated as:

$$\eta = \frac{C_0 - C_t}{C_0} \times 100$$

where C_0 and C_t were initial and final concentrations after a certain reaction time, respectively.

3 Results and discussion

In this work, we have improved an eco-friendly, pure, nontoxic method, for the generation of CuO NPs using the *B. ciliata* rhizome extract. (Fig. 1). *B. ciliata* is widely used in traditional medicine because of its

phytochemicals (bergenin, gallic acid, (+) - catechin, paa-shaanolactone, etc.). CuSO₄·5H₂O, initially metal precursor, reacts with the hydroxyl ion in water to form copper hydroxide. The phytochemicals contained in the *B. ciliata* extract are used as reducing and stabilizing agents. CuO NPs are synthesized from copper hydroxide with these phytochemicals.

3.1 Characterization of nanoparticles

The first step in the characterizing of NPs is the color transformation of solution (Fig. 2) indicating the reduction of copper ions into CuO NPs using an aqueous extract of *B. ciliata*. It occurs because of visual color change of solution from light brown to brick red (brownish), which is due to the excitation of surface plasmon vibrations in CuO NPs [20].

UV–Visible absorption spectrum was used for the analysis of optical properties of CuO NPs. Surface plasmon absorption of metal oxide generated an absorption peak at 260 nm in the spectrum. No additional peaks were found in the range of 200–700 nm, and the absorption peak was found to be symmetric. (Fig. 3a). The results were in good agreement with study of Kumar et al. [21]. Surface plasmon absorption and collective oscillation of free conduction band electrons stimulated by electromagnetic radiation are achieved in metal oxide NPs. If the wavelength of the incident light is greater than the particle diameter, resonance will occur. Surface plasma resonance absorbance is sensitive to the size and shape of the particles, their distance between particles, the surrounding environments and nature [22]. The BET surface area of the synthesized CuO nanoparticles by *B. ciliata* rhizome extract was found ~ 24 m² g⁻¹. Mahmoud et al. reported that it was ~ 20 m² g⁻¹ with a size of approximately 150 nm in their green synthesis study [23]. Another study found that the BET surface area of CuO NPs prepared with the same technique was 1.7 m² g⁻¹ with dimensions of 140 and 180 nm [24]. In the range of 4000–400 cm⁻¹, the FTIR spectrum was measured in the solid phase using the potassium bromide pellet technique. Figure 3b gives information about the spectral peaks proposing, the occurrence of bands relevant to amide N–H stretching (3402 cm⁻¹), amide C=O stretching (1578 cm⁻¹), alkanes C=O stretching (2350 cm⁻¹), nitro N–O bending (1399 cm⁻¹). The presence of CuO NPs band at 618 cm⁻¹ is assigned to the vibrations of Cu–O. The above result confirms that the bio-active compounds present in the *B. ciliata* rhizome extract have the upper hand in the production of CuO NPs. The little diversity in the peak position from original bonding shows that some of the metabolites (tannins, flavonoids, alkaloids, and carotenoids, etc.) are plenty in the bud extract that can produce the CuO NPs [25].

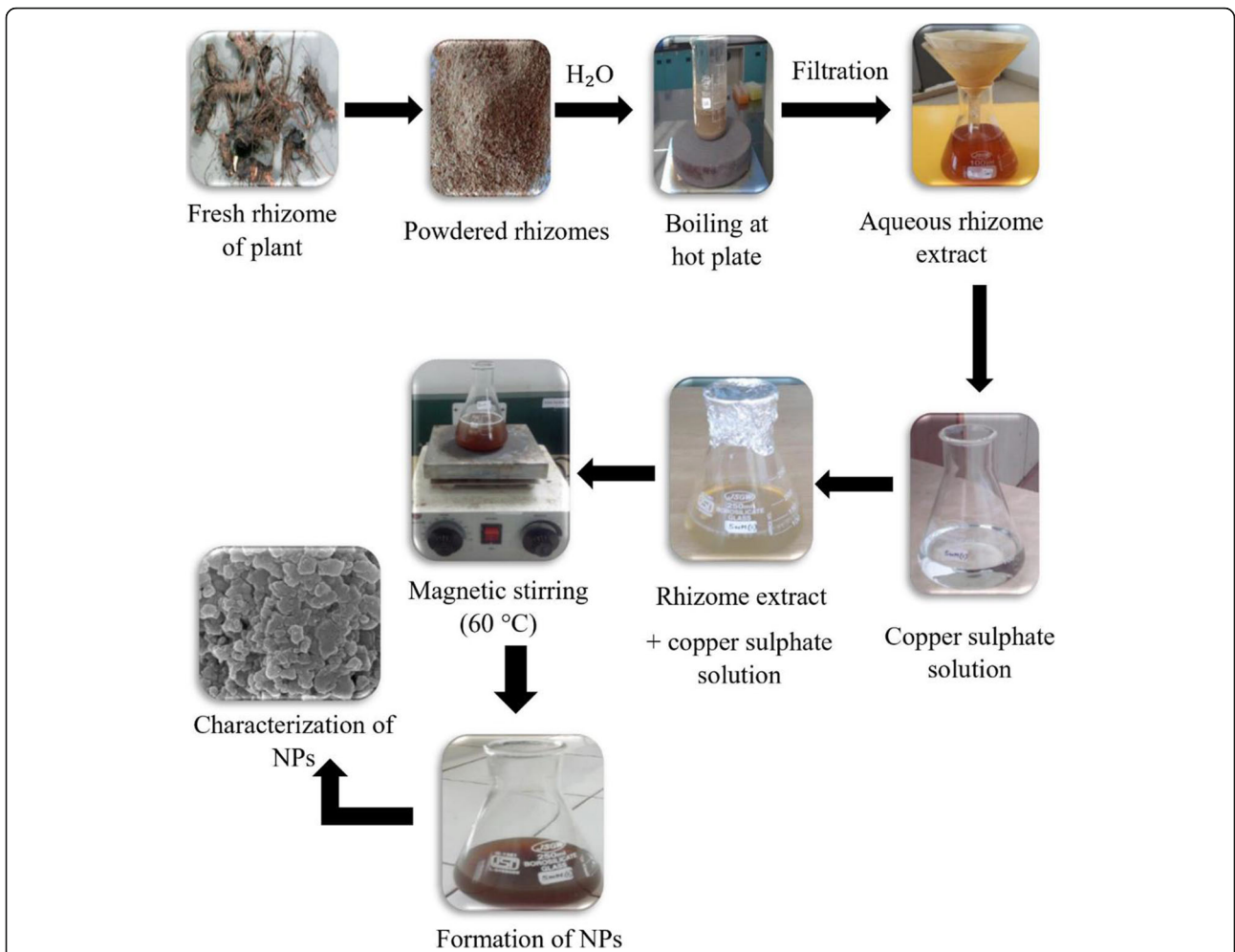


Fig. 1 Schematic of plant-mediated CuO NPs synthesis

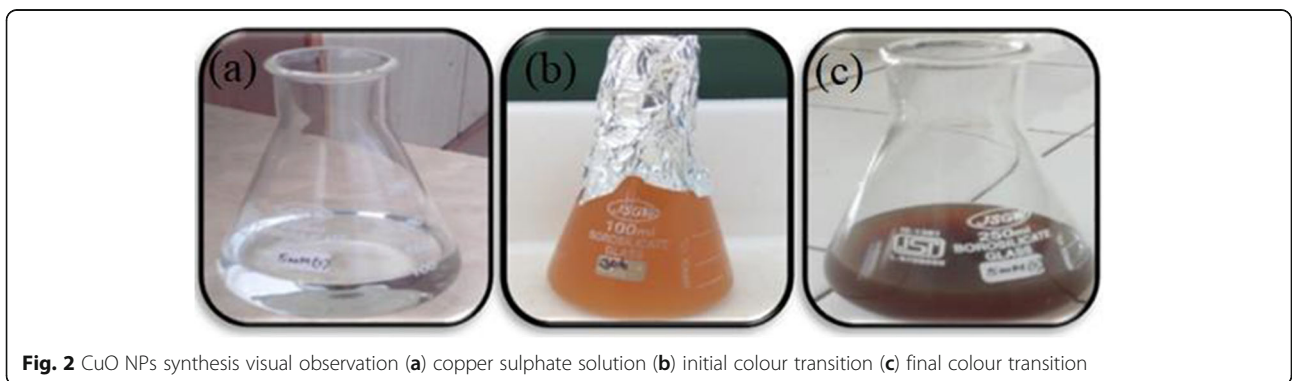
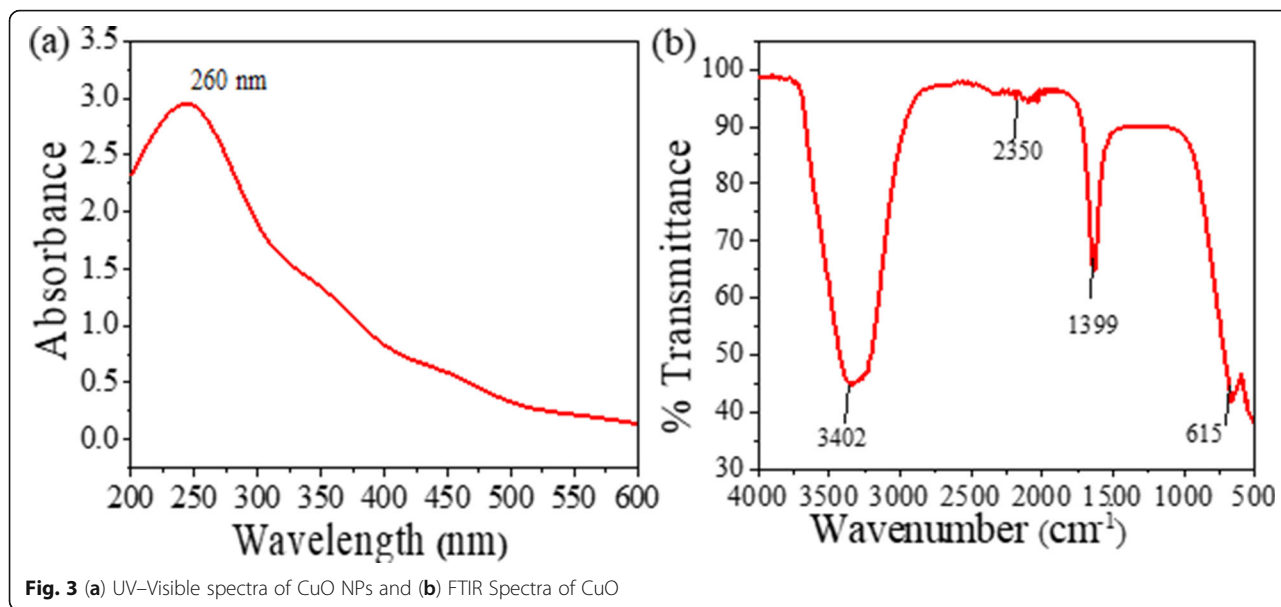


Fig. 2 CuO NPs synthesis visual observation (a) copper sulphate solution (b) initial colour transition (c) final colour transition

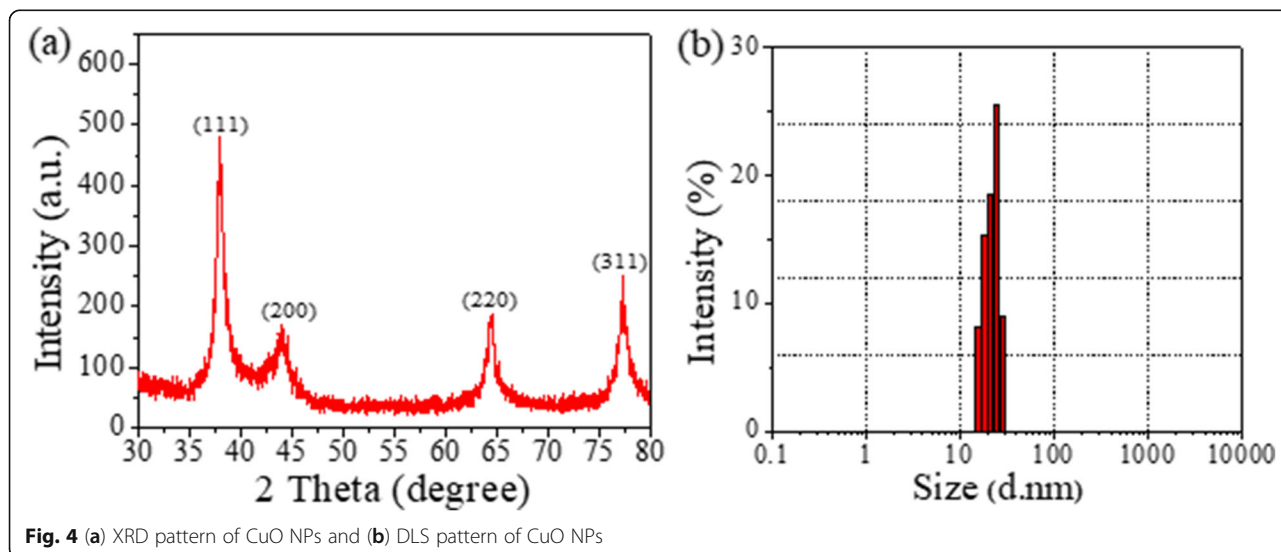


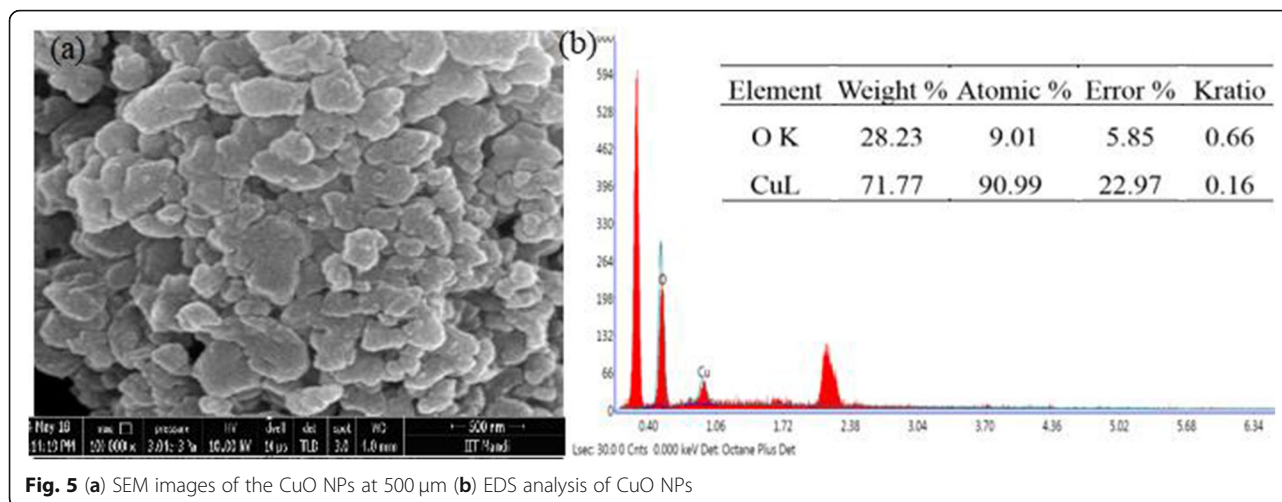
XRD analysis is used to determine the crystalline properties of NPs. In this work, XRD analysis of CuO NPs obtained by green synthesis is shown in Fig. 4a. Small different diffraction peaks at 32.80, 39.75, 61.40 and 71.02, that indexed the planes 111, 200, 220 and 311 of face centered cubic structure of CuO NPs with a monoclinic phase (JCPDS- 87-0717). CuO NPs synthesized from *B. ciliata* rhizome extract have been shown to be crystalline in nature by XRD analysis and no other phase shows that the purity of these NPs has been observed. The Debye-Scherrer equation was used to measure the crystal size of the NPs obtained [26]:

$$D = K\lambda/\beta\cos\theta$$

K: Scherrer's constant ($K = 0.94$), D: crystalline size, λ : X-ray wavelength (0.1546 nm), β : full width at half-maximum of the XRD line in radians and ' θ ' is the Bragg angle.

The average size of CuO NPs was measured to be about 20 nm. The XRD data of the bio-synthesis CuO NPs obtained in previous studies are parallel to the CuO NPs data obtained in this study. DLS analysis was used to measure the average particle size (Fig.





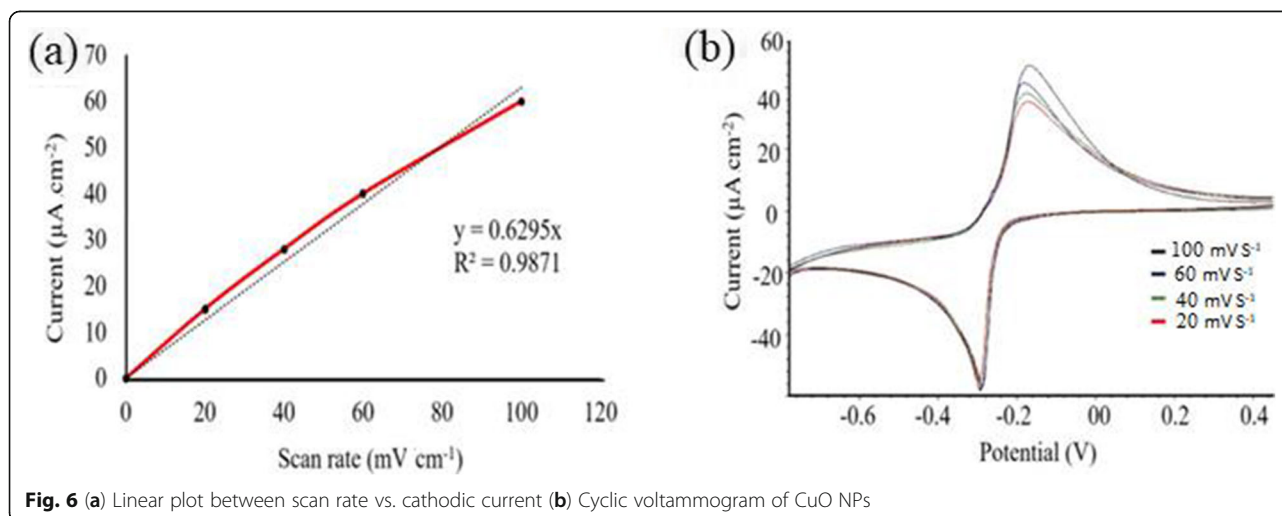
4b). The average particle size of the CuO NPs obtained accordingly is less than 50 nm. Figure 5a shows the SEM analysis of CuO NPs synthesized from *B. ciliata*. According to this SEM analysis, particles appear spherical and hexagonal, but there are also large particles formed by the combination of small particles. EDS analysis of CuO NPs synthesized by *B. ciliata* is given in Fig. 5b. According to this analysis, elemental Cu is at a highly intensive important peak of elemental Cu and O with the atomic 71.8% of and 28.2% which is in suitability with the main description line of metallic CuO NPs.

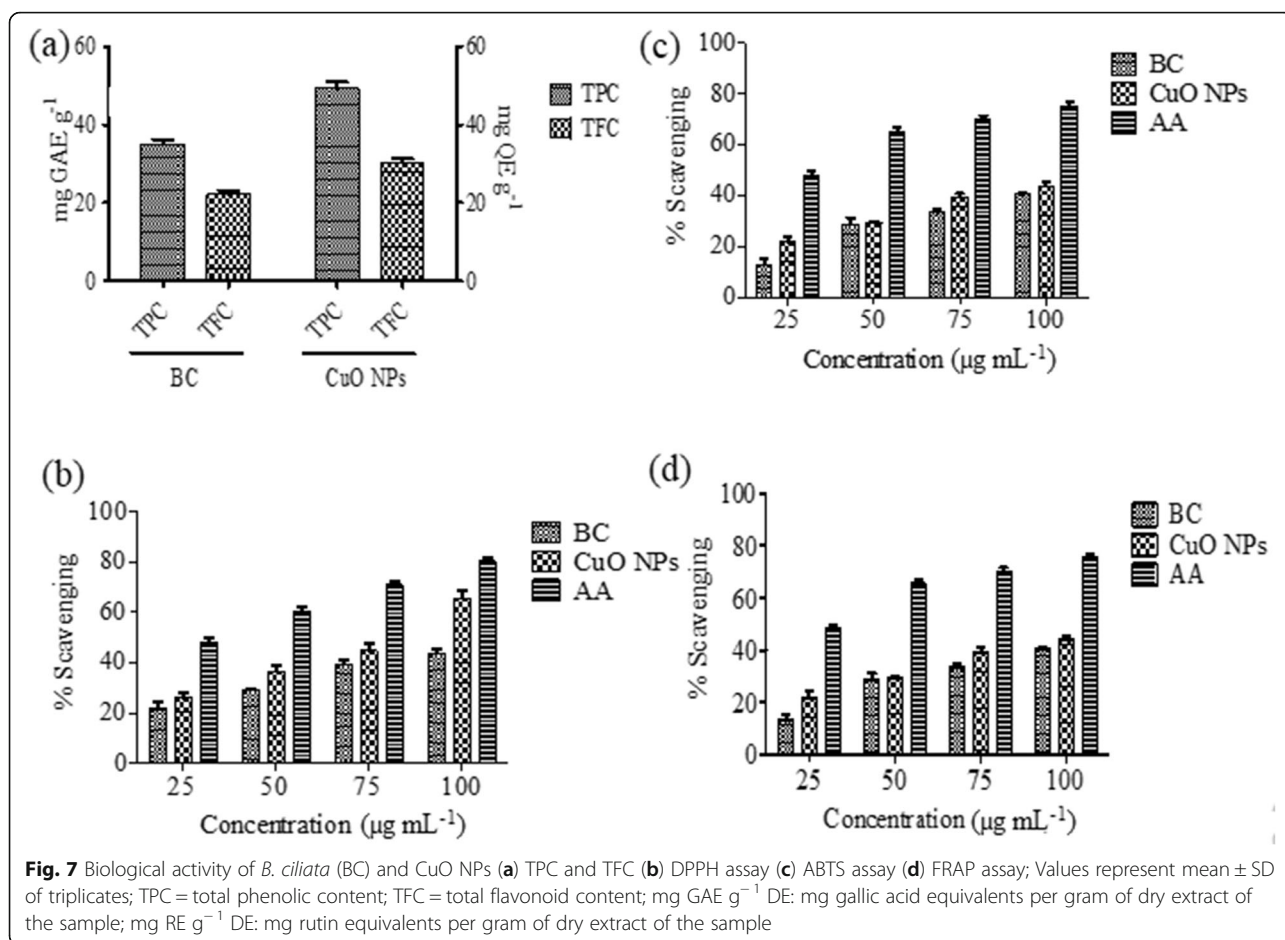
Consecutive increase in redox reaction, i.e., oxidation as well as reduction peaks were observed with increasing scan rate potential. Observing cathodic current peaks, i.e., 15 μA at 20 mV cm^{-1} , 28 μA at 40

mV cm^{-1} , 40 μA at 60 mV cm^{-1} and 60 μA at 100 mV cm^{-1} , indicating increased amount of catalytic activity due to presence of green synthesized CuO NPs. A linear plot between scan rate vs. cathodic current peaks is indicated in Fig. 6a and b. Scan rate range from 20 to 100 mV were used. Increase in scan rate corresponded to increase in cathodic current suggesting that CuO NPs electrode reduction is exclusively diffusion-controlled electron transfer and exhibits a strong linear relationship between current and scan rate with an R^2 value of 0.9871.

3.2 Antioxidant activity

Both the crude plant extract and the NPs were tested for phenolic and flavonoid content. Phenol content of *B. ciliata* was found to be $35.0 \pm 1.2 \text{ mg GAE g}^{-1}$. In





CuO NPs synthesised from the extract, this quantity is 49.2 ± 1.7 mg GAE g^{-1} . The bound flavonoid content of CuO NPs was measured (22.1 ± 1.0 mg QE g^{-1}). In *B. ciliata* extract contained 30.1 ± 1.3 mg QE g^{-1} of flavonoid material (Fig. 7a and Table 1).

Antioxidants are compounds that prevent the oxidation of essential biological macromolecules by inhibiting the propagation of the oxidizing chain reaction. The antioxidant activity of biogenic synthesis of CuO NPs was assessed using the DPPH, ABTS, and FRAP

Table 1 Antioxidant activity of *B. ciliata* and CuO NPs

Sample	ABTS	DPPH	FRAP
<i>B. ciliata</i>	138.0	135.2	144.1
CuO NPs	91.3	72.4	109.0
AA	28.7	29.2	26.3

DPPH = 2,2-diphenyl-1-picrylhydrazyl; ABTS = (2,2'-azino-bis (3-ethylbenzothiazoline-6-sulfonic acid); AA = Ascorbic acid; FRAP = Fe^{2+} -tripirydyltriazine

scavenging assays, which showed that a compound's reducing power is directly proportional to its antioxidant activity. CuO NPs is found to have antioxidant properties. For DPPH, CuO NPs ($IC_{50} = 91.2$ μg mL^{-1}), ABTS assays the CuO NPs ($IC_{50} = 72.4$ μg mL^{-1}) and FRAP assays the CuO NPs ($IC_{50} = 109$ μg mL^{-1}) (Fig. 7b,c and d). For the DPPH, ABTS, and FRAP assays, Ascorbic acid was used as a standard, IC_{50} values of 29.3, 28.7, and 26.3 μg mL^{-1} , respectively. This study reveals that *B. ciliata* and CuO NPs are more effective at scavenging free radicals and can be used as a major antioxidant source in antioxidant-based therapies. The CuO NPs' scavenging behaviour increases as the sample concentrations increase. As compared to other green synthesised NPs, the presence of proteins and amino acids, as well as carbohydrates, flavonoids, glycosides, phenolic compounds, saponins, and tannins, results in higher performance. The lower the IC_{50} value, the greater is the hydrogen donating potential of the free radical scavengers and thus their antioxidant activity.

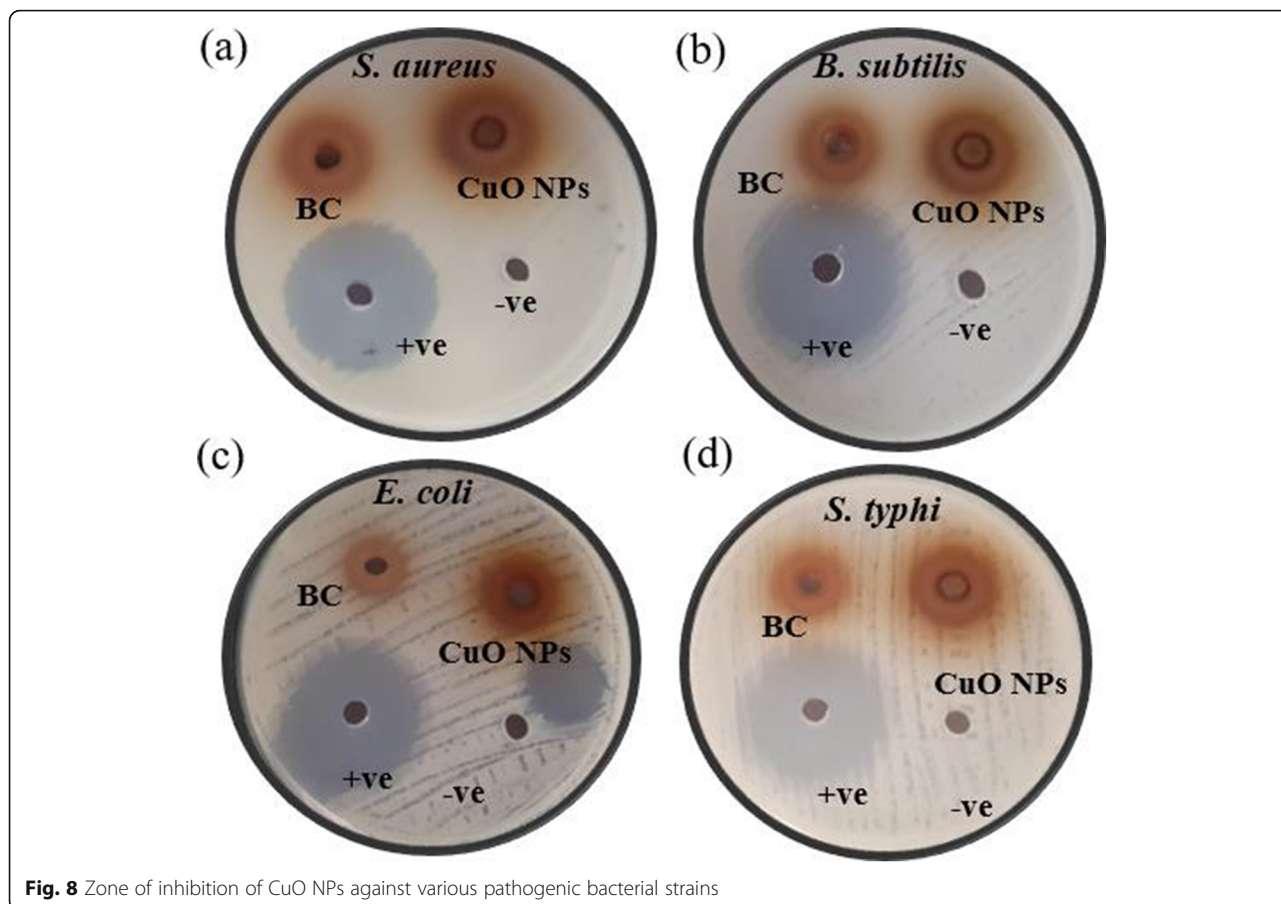


Fig. 8 Zone of inhibition of CuO NPs against various pathogenic bacterial strains

3.3 Antimicrobial activity

NPs have larger surface areas compared to large particles [27]. This large surface area interacts more with microorganisms, providing a high amount of antimicrobial effects. Copper, which has been used as an antibacterial factor for a long time, has a high antibacterial effect of 99.9% [28]. The antimicrobial effect of CuO NPs, which were synthesized by performing various optimizations, was investigated. According to the results of the agar well diffusion assay, the antimicrobial activity of 20 mg mL⁻¹ CuO NPs is effective

against food pathogens. Results revealed that the CuO NPs was better effective against all two Gram positive (*B. subtilis*, *S. aureus*) as compared to Gram negative (*E. coli*, *S. typhi*) bacterial strains shown in Fig. 8 and Table 2. On the basis of these observations, it can be concluded that synthesised CuO NPs had strong antibacterial activity against bacteria belonging to both Gram classes. CuO NPs have an important antibacterial property due to their large surface area, which helps them to make closer contact with microorganisms. By cross-linking within and between nucleic

Table 2 Zone of inhibition of CuO NPs against various pathogenic bacterial strain

Bacterial Strains	<i>B. ciliata</i>	CuO NPs	Positive control (Ampicillin-100 mg mL ⁻¹)	Negative control (dw)
<i>S. aureus</i>	13.5 ± 0.5	17.8 ± 0.4	23.8 ± 0.8	ND
<i>B. subtilis</i>	12.2 ± 0.7	15.8 ± 0.8	25.6 ± 1.6	ND
<i>E. coli</i>	7.5 ± 0.5	11.5 ± 0.5	25.6 ± 0.6	ND
<i>S. typhi</i>	10.3 ± 0.7	15.0 ± 1.2	23.3 ± 0.6	ND

Zones of inhibition (mm) are presented as mean ± SD. *S. aureus* = *Staphylococcus aureus*; *B. subtilis* = *Bacillus subtilis*; *E. coli* = *Escherichia coli*, *S. typhi* = *Salmonella typhi*. Amp = Ampicillin (positive control); ND (not detected)

Table 3 Minimum inhibitory concentration (MIC) of *B. ciliata*, CuO NPs and various pathogenic bacterial strain

MIC ($\mu\text{g mL}^{-1}$)			
No.	Bacteria	<i>B. ciliata</i>	CuO NPs
1	<i>B. subtilis</i>	25	6.25
2	<i>S. aureus</i>	25	6.25
3	<i>E. coli</i>	25	6.25
4	<i>S. typhi</i>	50	12.5

acid strands, copper ions released later can bind with DNA molecules, causing helical structure disorder. Biochemical processes are often affected by copper ions in bacterial cells [29]. The exact mechanism behind is not known and needs to be studied further. Furthermore, the Gram negative bacteria seemed to be more resistant to CuO NPs than Gram positive bacteria [30]. It was earlier reported that the interaction between Gram positive bacteria and NPs was stronger than that of Gram negative bacteria because of the difference in cell walls between Gram positive and Gram negative bacteria. *B. ciliata* and CuO NPs were used to inhibit the growth of test organisms as described. The MIC was found to be $6.25 \mu\text{g mL}^{-1}$ against *S. aureus*, *B. subtilis*, *S. typhi* and $25 \mu\text{g mL}^{-1}$ against *E. coli* (Table 3).

3.4 Photocatalytic degradation

Figure 9 depicts the dye degradation mechanism followed by CuO NPs. Sharma and Dutta reported that hydroxy radicals were the most important reactive oxygen species that caused degradation when CuO NPs were used [31]. CuO NPs have been widely used as catalysts in photocatalytic degradation and reduction of contaminants [32]. In fact, dark adsorption is an initial step and one of the most critical aspects of the photocatalysis mechanism [33]. CuO NPs were used to study the photo degradation of cationic dyes like MB and MR when exposed to sunlight. In the presence of light radiation, the MB and MR solutions were stirred in the dark for 1 h to establish adsorption–desorption equilibrium between the CuO NPs and dye molecules. A UV–Visible spectrum was then used to estimate the MB and MR concentrations. Within 135 min, the photocatalytic activity of *B. ciliata* rhizome extract mediated CuO NPs and the absorption peaks at 625 and 525 nm decreased, comprising MB and MR dye (Fig. 9a and b). The morphology, crystalline structure, and dimensions of NPs all play a role in photocatalytic activity. Control experiments were carried out in the dark (both with and without CuO NPs) to rule out any possibility of dye

self-degradation, dye adsorption, or NP catalytic activity in the dark. In the absence of CuO NPs, we observed negligible dye degradation after the experiment was completed (Fig. 9c and d). Similarly, CuO NPs had a negligible effect on dye degradation in the dark. As a result, it was determined that the dyes did not degrade significantly in dark conditions. Furthermore, dye degradation experiments in the absence of a catalyst revealed negligible dye degradation. MB and MR, on the other hand, were nearly fully degraded under direct sunlight in the presence of catalyst. Sunlight is a very important factor from an industrial perspective. The degradation was 55, 47%, for MB and MR dyes, respectively within 75 min of photo irradiation. While it was 92, 85% for MB and MR dyes, respectively within 135 min of photo irradiation. After 3 h of irradiation, an efficiency of 92 and 85% is obtained, indicating that integrating CuO NPs species into the solution serves a primary function in the improvement of photodegradation, as shown (Fig. 9e). The degradation of MB dye was observed higher as compared to MR dyes.

The related compounds and structural formulae could be interpreted based on the mass/charge ratios in the mass spectra, as illustrated in Fig. 10a (MB) and Fig. 10b (MR). The photocatalytic breakdown route of MB and MR can also be investigated at the same time. During the photocatalytic decomposition of MB and MR, certain intermediate compounds were generated by demethylation. Mass spectra were used to identify all of the intermediate compounds produced during photocatalytic decomposition of MB and MR. As a result, utilizing CuO nanoparticles for photocatalysis to purify MB and MR is a green and efficient technique.

It has been reported that the catalytic activity of a nano-catalyst is strongly influenced by the morphology and size of NPs, as well as the process of energy transfer, photo-generated carriers generation and consumption. Balakumaran et al. [34] used Sn_3O_4 NPs to demonstrate the same form of degradation of MB dye within 60 min under sunlight irradiation. Sonia et al. [35] degraded the MB dye in 180 min using CuO NPs.

3.5 Mechanisms

Figure 11 illustrates the mechanism for photocatalytic activity. By generating holes in the valence band, a source of light induces electrons to excite from the valence to the conduction band. The photocatalyst holes oxidise the H_2O molecules in the reaction sample to more reactive OH radicals. Owing to the presence of excited electrons in the CB, the oxygen molecule gets reduced to O^{-2} radicals, and H_2O_2 gets

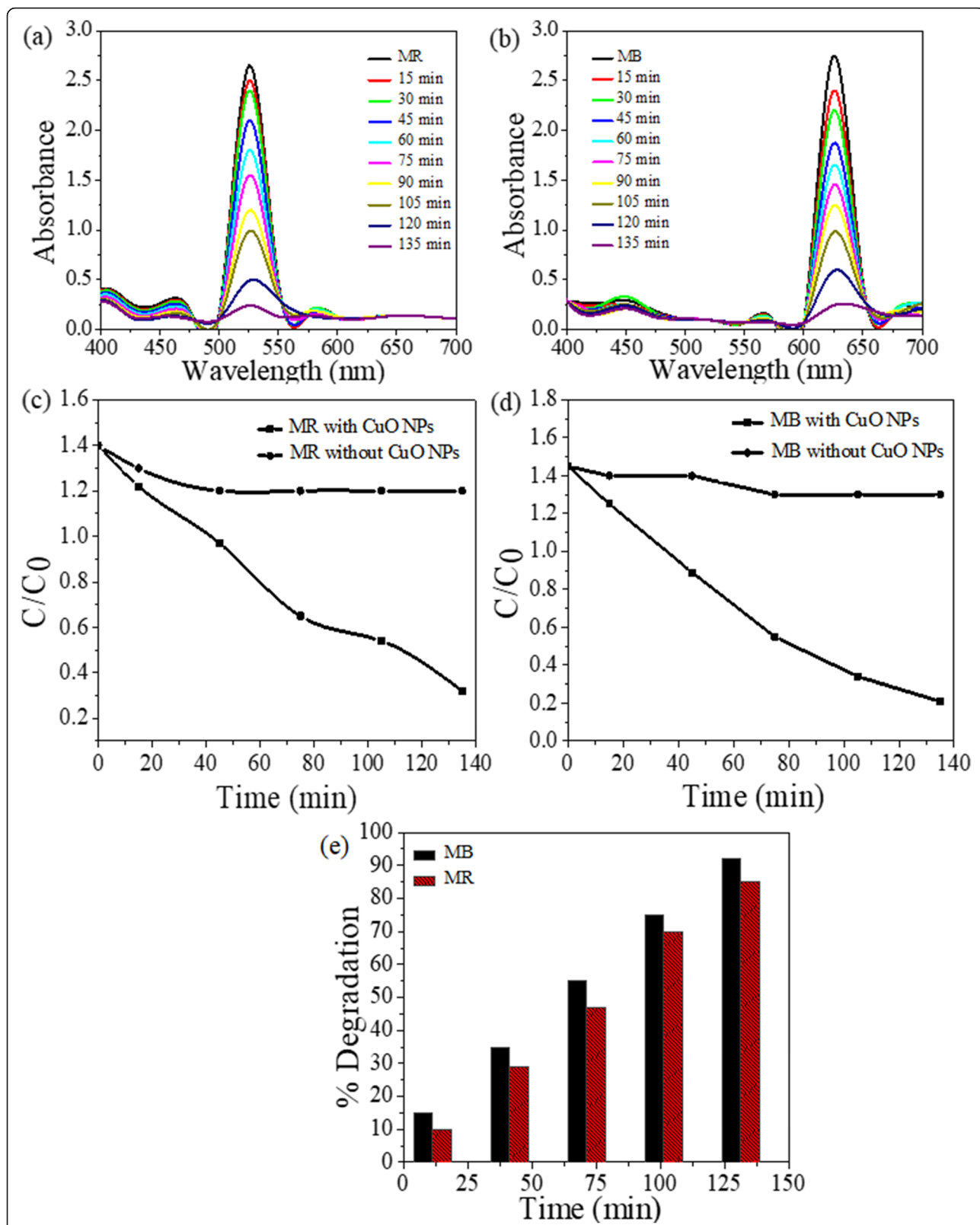
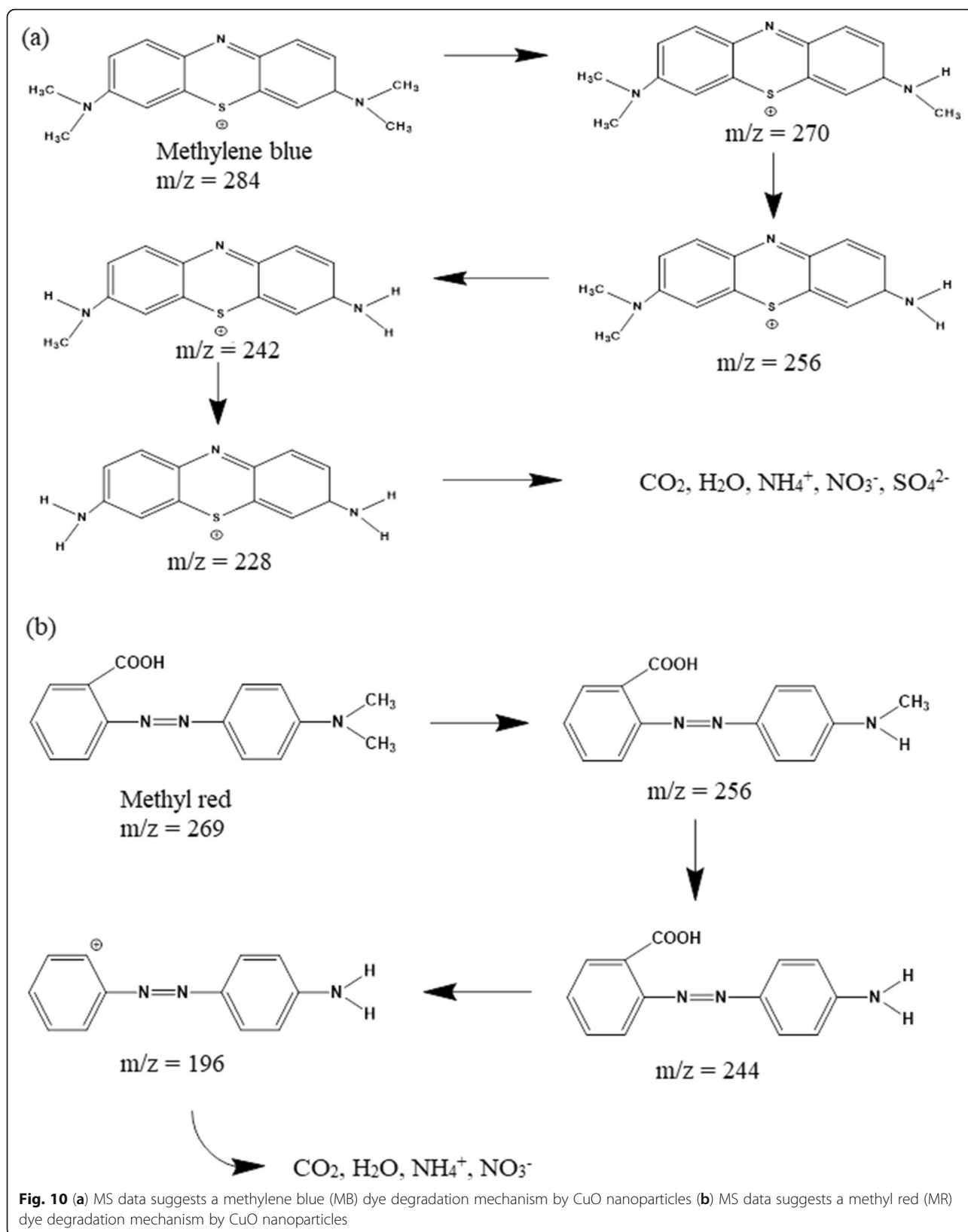
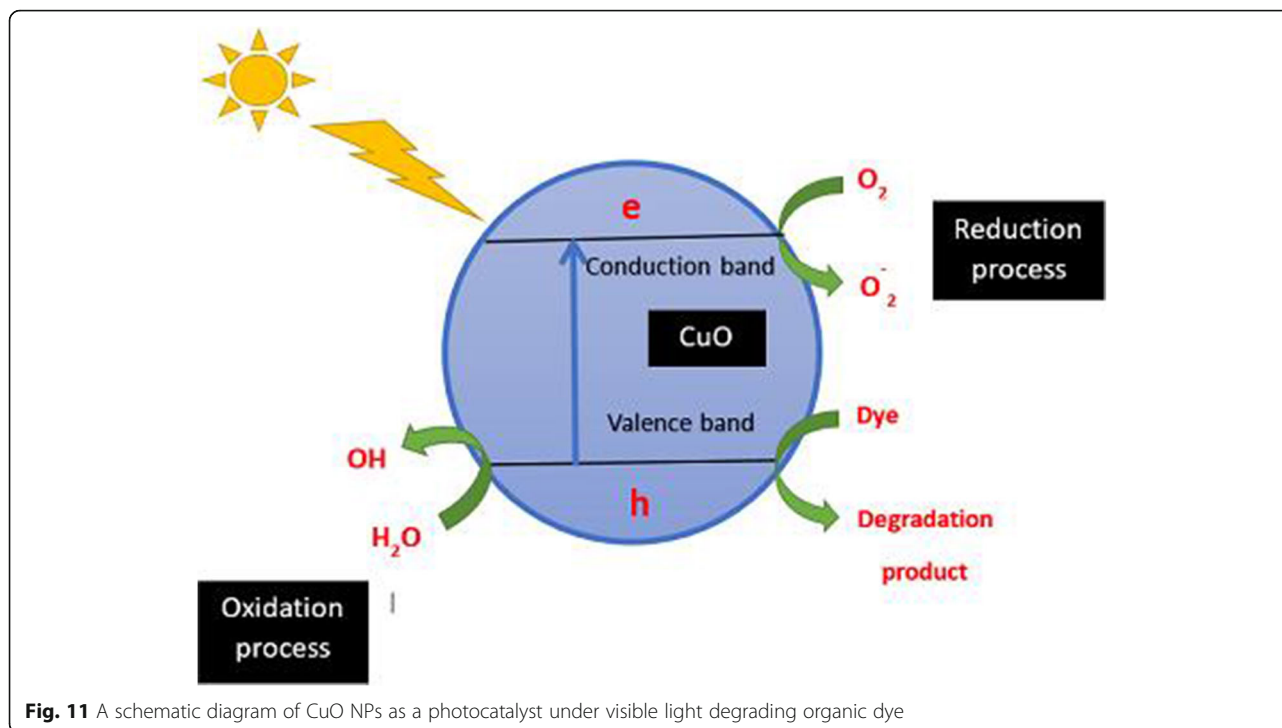


Fig. 9 UV- visible spectra of CuO NPs during dye degradation (a) MB under sunlight (b) and MR under sunlight; (c) MB (d) MR, degradation of dyes in the dark and under sunlight in the absence and presence of catalyst; (e) the photocatalytic degradation of CuO NPs, methylene blue (MB) and methyl red (MR) dyes under sunlight





reduced to OH radicals. The oxidative decomposition of dye to CO_2 , H_2O , and other mineralization products can be caused by the oxide and hydroxyl radicals formed by CuO NPs [36]. The study also observed from Table 4 that the current approach gave a very good dye degradation when compared with other photocatalysts.

4 Conclusions

In conclusion, using the medicinal plant *B. ciliata* as a reducing and stabilizing agent, the synthesis of CuO nanoparticles was carried out in a simple and environmentally friendly way. While the synthesis of different nanoparticles was carried out with *B. ciliata* in different previous studies, the green synthesis of CuO nanoparticles with *B. ciliata* was successfully reported for the first time in this study. The characteristic peak at 260 nm is noticeable in the UV–Visible

absorption range. Cu–O bonding was confirmed by FTIR spectra, and XRD patterns revealed monoclinic phase with an average grain size of 20 nm. The particles tend to be almost highly stable and spherical in form, according to SEM images. CuO NPs elemental composition was verified by EDX examination. Furthermore, the CuO NPs synthesized had a high level of activity against Gram positive bacteria (*S. aureus*). CuO NPs synthesised by the green method reveals substantial activity in in vitro antioxidant assays using various methods. Photocatalytic activity of CuO NPs against cationic dye has also been demonstrated. This is the first study on bio-inspired green synthesis of CuO NPs from *B. ciliata* rhizome extract, confirming their antimicrobial, antioxidant, and photocatalytic properties. Thus, it could pave a way for the futuristic synthesis of environmentally benign, cost-effective CuO NPs from medicinal plants.

Table 4 Comparative assessment of dyes degradation efficiency using different photocatalysts

NPs	Dye	Catalyst concentration	Dye concentration (mg L^{-1})	Time (min)	% degradation	Reference
CuO	Congo red	1 mg mL^{-1}	10	60	90	[37]
	Nile blue (NB)	40 ppm	1	120	93	[38]
ZnO	MV6B	0.50 g	100	210	68	[39]
	Reactive black 5	3 g L^{-1}	496	60	60	[40]
CuO	MB	20 ppm	10	135	92	Present study
	MR	20 ppm	10	135	85	

Acknowledgments

The authors acknowledge Vice-Chancellor, Shoolini University, Solan, for providing infrastructure support to conduct the research work. Authors are highly thankful to the School of Bioengineering and Food Technology, Shoolini University, Solan, India.

Authors' contributions

K. Dulta conceptualised the study, designed the methods, conducted experiments, wrote the first and revised draft. G. K. Ağçeli, P. Chauhan and R. Jasrotia conducted experiments. P. K. Chauhan supervised the study and worked on the revised draft. J. O. Ighalo assisted in data interpretation and worked on the revised draft. All authors read and approved the final manuscript.

Funding

This research did not receive external funding.

Availability of data and materials

The raw data is available by contacting the authors.

Declarations

Ethical approval

This article does not contain any studies with human participants or animals performed.

Competing interests

The authors declare that they have no conflict of interests.

Author details

¹Faculty of Applied Sciences and Biotechnology, Shoolini University, Solan 173229, India. ²Department of Biology/Biotechnology, Hacettepe University, 06800 Ankara, Turkey. ³Faculty of Physics and Material Science, Shoolini University, Solan 173229, India. ⁴Department of Chemical Engineering, Nnamdi Azikiwe University, Awka 420007, Nigeria. ⁵Department of Chemical Engineering, University of Ilorin, Ilorin 240003, Nigeria.

Received: 27 May 2021 Accepted: 29 November 2021

Published online: 06 January 2022

References

- Li CL, Tan HB, Lin JJ, Luo XL, Wang SP, You J, et al. Emerging Pt-based electrocatalysts with highly open nanoarchitectures for boosting oxygen reduction reaction. *Nano Today* 2018;21:91–105.
- Ighalo JO, Sagboye PA, Umenweke G, Ajala OJ, Omoarukhe FO, Adeyanju CA, et al. CuO nanoparticles (CuO NPs) for water treatment: a review of recent advances. *Environ Nanotechnol Monit Manage* 2021;15:100443.
- Ali M, Kim B, Belfield KD, Norman D, Brennan M, Ali GS. Green synthesis and characterization of silver nanoparticles using *Artemisia absinthium* aqueous extract – a comprehensive study. *Mat Sci Eng C-Mater* 2016;58:359–65.
- Das SK, Dickinson C, Lafir F, Brougham DF, Marsili E. Synthesis, characterization and catalytic activity of gold nanoparticles biosynthesized with *Rhizopus oryzae* protein extract. *Green Chem* 2012;14:1322–34.
- Arruda SCC, Silva ALD, Galazzi RM, Azevedo RA, Arruda MAZ. Nanoparticles applied to plant science: a review. *Talanta* 2015;131:693–705.
- Suarez-Cerda J, Espinoza-Gomez H, Alonso-Nunez G, Rivero IA, Gochi-Ponce Y, Flores-Lopez LZ. A green synthesis of copper nanoparticles using native cyclodextrins as stabilizing agents. *J Saudi Chem Soc* 2017;21:341–8.
- Tadjarodi A, Roshani R. A green synthesis of copper oxide nanoparticles by mechanochemical method. *Curr Chem Lett* 2014;3:215–20.
- Chang YN, Zhang MY, Xia L, Zhang J, Xing GM. The toxic effects and mechanisms of CuO and ZnO nanoparticles. *Materials* 2012;5:2850–71.
- Rajkumar V, Guha G, Kumar RA, Mathew L. Evaluation of antioxidant activities of *Bergenia ciliata* Rhizome. *Rec Nat Prod* 2010;4:38–48.
- Saha S, Verma RJ. Inhibition of calcium oxalate crystallisation *in vitro* by an extract of *Bergenia ciliata*. *Arab J Urol* 2013;11:187–92.
- Sankar R, Manikandan P, Malarvizhi V, Fathima T, Shivashangari KS, Ravikumar V. Green synthesis of colloidal copper oxide nanoparticles using *Carica papaya* and its application in photocatalytic dye degradation. *Spectrochim Acta A* 2014;121:746–50.
- Ighalo JO, Adeniyi AG. A mini-review of the morphological properties of biosorbents derived from plant leaves. *SN Appl Sci* 2020;2:509.
- Singleton VL, Rossi JA. Colorimetry of total phenolics with phosphomolybdic-phosphotungstic acid reagents. *Am J Enol Vitic* 1965;16:144–58.
- Meda A, Lamien CE, Romito M, Millogo J, Nacoulma OG. Determination of the total phenolic, flavonoid and proline contents in Burkina Faso honey, as well as their radical scavenging activity. *Food Chem* 2005;91:571–7.
- Re R, Pellegrini N, Proteggente A, Pannala A, Yang M, Rice-Evans C. Antioxidant activity applying an improved ABTS radical cation decolorization assay. *Free Radical Bio Med* 1999;26:1231–7.
- Barros L, Ferreira MJ, Queiros B, Ferreira ICFR, Baptista P. Total phenols, ascorbic acid, beta-carotene and lycopene in Portuguese wild edible mushrooms and their antioxidant activities. *Food Chem* 2007;103:413–9.
- Benzie IFF, Strain JJ. The ferric reducing ability of plasma (FRAP) as a measure of "antioxidant power": the FRAP assay. *Anal Biochem* 1996;239:70–6.
- Perez C, Pauli M, Bazerque P. An antibiotic assay by the agar well diffusion method. *Acta Biol Med Exp* 1990;15:113–5.
- Dulta K, Ağçeli GK, Chauhan P, Jasrotia R, Chauhan PK. A novel approach of synthesis zinc oxide nanoparticles by *Bergenia ciliata* rhizome extract: antibacterial and anticancer potential. *J Inorg Organomet Polym* 2020;31:180–90.
- Kriithiga N, Jayachitra A, Rajalakshmi A. Synthesis, characterization and analysis of the effect of copper oxide nanoparticles in biological systems. *Indian J Nanosci* 2013;1:6–15.
- Kumar PPNV, Shameem U, Kollu P, Kalyani RL, Pammi SVN. Green synthesis of copper oxide nanoparticles using aloe vera leaf extract and its antibacterial activity against fish bacterial pathogens. *Bionanoscience* 2015;5:135–9.
- Jain PK, Huang X, El-Sayed IH, El-Sayed MA. Review of some interesting surface plasmon resonance-enhanced properties of noble metal nanoparticles and their applications to biosystems. *Plasmonics* 2007;2:107–18.
- Mahmoud AE, Al-Qahtani KM, Alflajj SO, Al-Qahtani SF, Alsamhan FA. Green copper oxide nanoparticles for lead, nickel, and cadmium removal from contaminated water. *Sci Rep-UK* 2021;11:12547.
- Baylan N, Ilalan I, Inci I. Copper oxide nanoparticles as a novel adsorbent for separation of acrylic acid from aqueous solution: synthesis, characterization, and application. *Water Air Soil Poll* 2020;231:465.
- Ren GG, Hu DW, Cheng EWC, Vargas-Reus MA, Reip P, Allaker RP. Characterisation of copper oxide nanoparticles for antimicrobial applications. *Int J Antimicrob Ag* 2009;33:587–90.
- Sangeetha G, Rajeshwari S, Venckatesh R. Green synthesis of zinc oxide nanoparticles by aloe barbadensis miller leaf extract: structure and optical properties. *Mater Res Bull* 2011;46:2560–6.
- Iwuozor KO, Ighalo JO, Ogunfowora LA, Adeniyi AG, Igwegbe CA. An empirical literature analysis of adsorbent performance for methylene blue uptake from aqueous media. *J Environ Chem Eng* 2021;9:105658.
- Hajjipour MJ, Fromm KM, Ashkaran AA, de Aberasturi DJ, de Larramendi IR, Rojo T, et al. Antibacterial properties of nanoparticles. *Trends Biotechnol* 2012;30:499–511.
- Kim JH, Cho H, Ryu SE, Choi MU. Effects of metal ions on the activity of protein tyrosine phosphatase VHR: highly potent and reversible oxidative inactivation by Cu²⁺ ion. *Arch Biochem Biophys* 2000;382:72–80.
- Emami-Karvani Z, Chehrizi P. Antibacterial activity of ZnO nanoparticle on gram-positive and gram-negative bacteria. *Afr J Microbiol Res* 2011; 5:1368–73.
- Sharma A, Dutta RK. Studies on the drastic improvement of photocatalytic degradation of acid orange-74 dye by TPPO capped CuO nanoparticles in tandem with suitable electron capturing agents. *RSC Adv* 2015;4:43815–23.
- Pradhan N, Pal A, Pal T. Silver nanoparticle catalyzed reduction of aromatic nitro compounds. *Colloid Surface A* 2002;196:247–57.
- Slama R, El Ghoul J, Ghiloufi I, Omri K, El Mir L, Houas A. Synthesis and physico-chemical studies of vanadium doped zinc oxide nanoparticles and its photocatalysis. *J Mater Sci-Mater El* 2016;27:8146–53.
- Balakumaran MD, Ramachandran R, Balashanmugam P, Mukeshkumar DJ, Kalaiichelvan PT. Mycosynthesis of silver and gold nanoparticles: optimization, characterization and antimicrobial activity against human pathogens. *Microbiol Res* 2016;182:8–20.

35. Sonia S, Poongodi S, Kumar PS, Mangalaraj D, Ponpandian N, Viswanathan C. Hydrothermal synthesis of highly stable CuO nanostructures for efficient photocatalytic degradation of organic dyes. *Mat Sci Semicon Proc* 2015;30: 585–91.
36. Patil SB, Naik HSB, Nagaraju G, Viswanath R, Rashmi SK. Synthesis of visible light active Gd³⁺-substituted ZnFe₂O₄ nanoparticles for photocatalytic and antibacterial activities. *Eur Phys J Plus* 2017;132:328.
37. Aminuzzaman M, Kei LM, Liang WH. Green synthesis of copper oxide (CuO) nanoparticles using banana peel extract and their photocatalytic activities. *AIP Conf Proc* 2017;1828:020016.
38. Singh J, Kumar V, Kim KH, Rawat M. Biogenic synthesis of copper oxide nanoparticles using plant extract and its prodigious potential for photocatalytic degradation of dyes. *Environ Res* 2019;177:108569.
39. Subhan MA, Awal MR, Ahmed T, Younus M. Photocatalytic and antibacterial activities of Ag/ZnO nanocomposites fabricated by co-precipitation method. *Acta Metall Sin-Engl* 2014;27:223–32.
40. Amisha S, Selvam K, Sobana N, Swaminathan M. Photomineralisation of Reactive Black 5 with ZnO using solar and UV-A light. *J Korean Chem Soc* 2008;52:66–72.

Publisher's Note

Springer Nature remains neutral with regard to jurisdictional claims in published maps and institutional affiliations.

Ready to submit your research? Choose BMC and benefit from:

- fast, convenient online submission
- thorough peer review by experienced researchers in your field
- rapid publication on acceptance
- support for research data, including large and complex data types
- gold Open Access which fosters wider collaboration and increased citations
- maximum visibility for your research: over 100M website views per year

At BMC, research is always in progress.

Learn more biomedcentral.com/submissions

